

1 **SUPPORTING INFORMATION**

2

3 **Spatially-directed Magnetic Molecularly Imprinted**
4 **Polymers with Good Anti-interference for Simultaneous**
5 **Enrichment and Detection of Dual Disease-related Bio-**
6 **indicators**

7 Huijia Song ^{a,†}, Feng Wang ^{a,†}, Yayun Zhao ^a, Ruixia Gao ^{*a}, Yulian He ^c, Qing Yan ^d,
8 Xiaoyi Chen ^d, Lisa D. Pfefferle ^e, Silong Xu ^a, Ying Sheng ^{*a,b}

9 ^a *School of Chemistry, Xi'an Jiaotong University, Xi'an, Shaanxi 710049, China*

10 ^b *Department of Otolaryngology Head and Neck Surgery, The Second Affiliated*
11 *Hospital of Xi'an Jiaotong University, Xi'an, Shaanxi 710004, China*

12 ^c *University of Michigan—Shanghai Jiaotong University Joint Institute, Shanghai*
13 *200240, China*

14 ^d *School of Medicine, Xi'an Jiaotong University, Xi'an, Shaanxi 710061, China*

15 ^e *Department of Chemical & Environmental Engineering, Yale University, New Haven,*
16 *Connecticut 06520-8286, United States*

17 † Huijia Song and Feng Wang contributed equally to this work and are co-first authors.

18 * Corresponding authors: Tel.: +86 29 82655399; fax: +86 29 82655399.

19 E-mail: ruixiagao@xjtu.edu.cn (R. Gao)

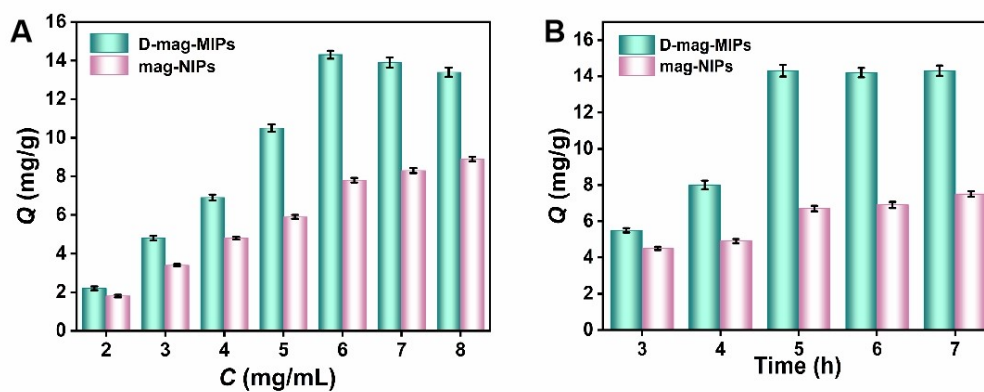
20 15229217817@163.com (Y. Sheng)

21

22 **1. Instrumentation**

23 Images of transmission electron microscopy were obtained using a JEM-2100
24 transmission electron microscope (TEM, JEOL Co., Japan). Hysteresis loops were
25 acquired by a 9600-1 vibrating sample magnetometer (VSM, LDJ Co., USA) for testing
26 the magnetic properties of resultant materials. X-ray diffraction patterns were recorded
27 with a Rigaku D/max/2500v/pc X-ray diffractometer (Rigaku Co., Japan) with Cu $K\alpha$
28 radiation to identify the crystalline phase of nanomaterials. A Nicolet AVATAR-330
29 Fourier-transform infrared spectrophotometer (FTIR) (Thermo Electron Co. USA) was
30 utilized by the KBr pressing method. An automatic elemental analyzer (EL,
31 EUROVECTOR EA3000, Italy) was used to obtain elemental contents. The HPLC
32 analyses were conducted using a Hitachi L-2130 HPLC system (Japan) equipped with
33 a binary pump, an ultraviolet detector, and a C18 chromatographic column (150
34 mm×4.6 mm, 5 μ m, Shimadzu, VP-ODS). The optimized mobile phase was
35 acetonitrile-ultrapure water (5:95, v/v) with regular flow rate of 0.5 mL/min and
36 injection volume of 10 μ L. The column temperature was 40 °C, and the detection
37 wavelength was operated at 283 nm.

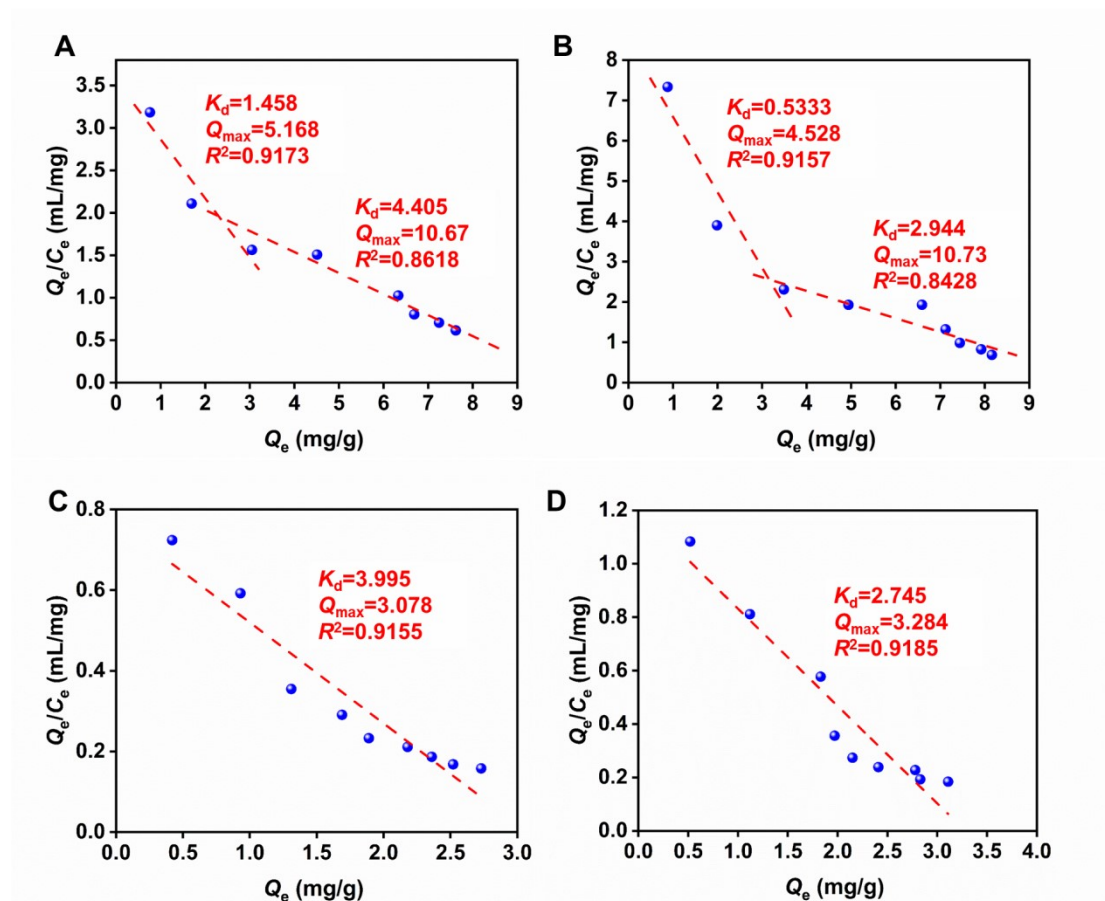
38



39

40 **Fig. S1.** The effect of the amount of PEI (A) and polymerization time (B) on the
 41 imprinting performance of D-mag-MIPs and mag-NIPs towards DOPAC.

42

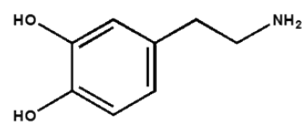


43

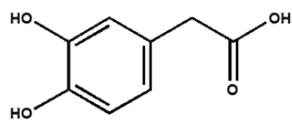
44 **Fig. S2.** Scatchard plots for D-mag-MIPs towards DA (A) and DOPAC (B). Scatchard
 45 plots for mag-NIPs towards DA (C) and DOPAC (D).

46

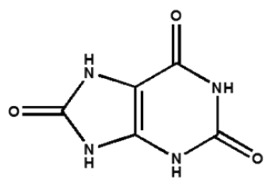
47



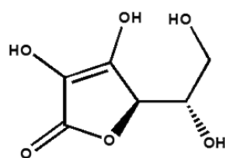
DA



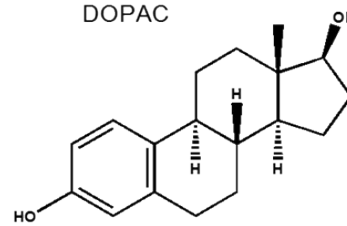
DOPAC



UA



AA

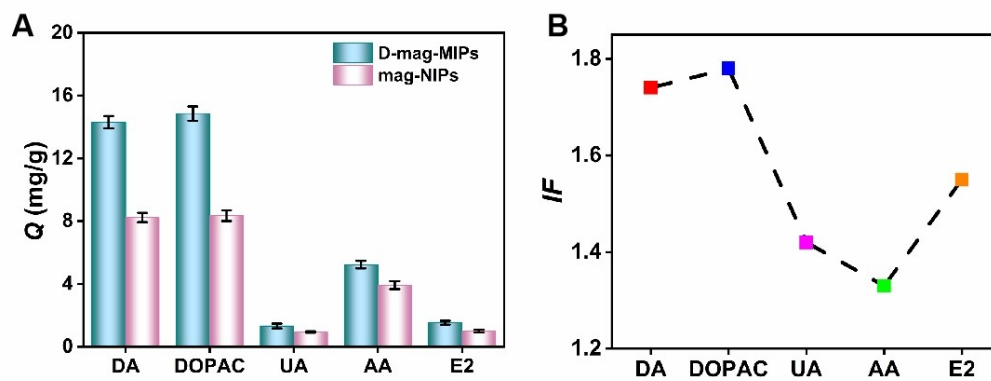


E2

48

49 **Fig. S3.** Chemical structures of DA, DOPAC, and their coexisting competitors.

50

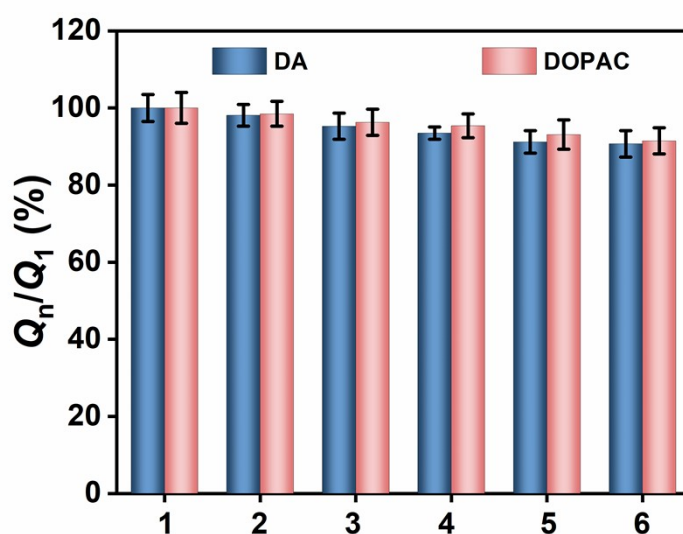


51

52 **Fig. S4.** Selective adsorption capacity (A) and IF (B) of D-mag-MIPs and mag-NIPs

53 towards different compounds in the single solutions.

54



55

56 **Fig. S5.** The reusability test of D-mag-MIPs after six adsorption-desorption cycles.

57 To assess the reusability, which is of great importance when it comes to transitioning

58 from lab scales to any realistic practical applications, we performed six adsorption-

59 desorption cycles on the same D-mag-MIPs (Fig. S5). The adsorption capacities of D-

60 mag-MIPs for DA and DOPAC show a slight decrease after 6 cycles, likely due to the

61 minor destruction of imprinted cavities caused by the ethanol-HAC (98:2, v/v) eluent

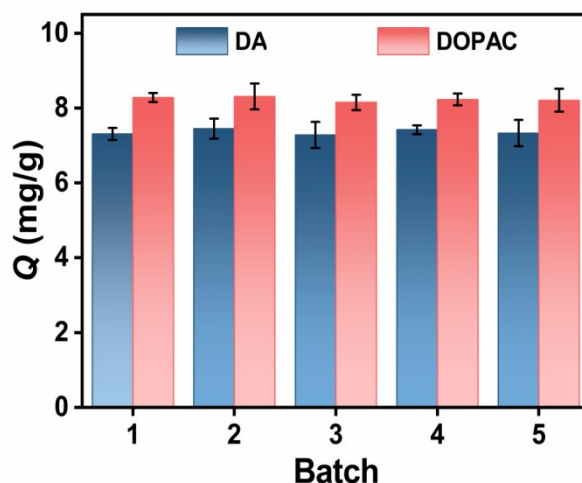
62 used to remove the adsorbed templates by disruption the interaction between templates

63 and functional monomer. However, it still maintains above 91% of the initial adsorption

64 amount, revealing that D-mag-MIPs are stable and possess good reusability in

65 applications.

66



67 **Fig. S6.** The reproducibility of D-mag-MIPs prepared in five batches.

68 To investigate the long-term utilization of D-mag-MIPs, the reproducibility of
69 obtained nanomaterials were tested. Five different batches of D-mag-MIPs were
70 synthesized on different days. The adsorption of DA and DOPAC on each batch of
71 nanomaterials was performed by five times independently (Fig. S6). The average Q
72 values of the different batches of D-mag-MIPs towards DA and DOPAC are found to
73 be 7.35 and 8.24 mg/g with RSD <5.5% and 6.2%, respectively. These results
74 demonstrate that D-mag-MIPs possess satisfactory reproducibility, indicating the
75 satisfactory stability of the prepared nanomaterials.

76

77 **Table S1** The adsorption kinetic constants for pseudo-first-order and pseudo-second-
 78 order rate kinetic models of D-mag-MIPs.

Sorbents	Targets	Pseudo-first-order		Pseudo-second-order		
		R^2	k_1 (/min)	R^2	k_2 (g/mg·min)	v_0 (mg/g·min)
D-mag-MIPs	DA	0.8631	0.5977	0.9563	0.0296	3.292
	DOPAC	0.9068	0.5370	0.9775	0.0473	5.030

79

80

81 **Table S2.** Adsorption equilibrium constants for *Langmuir* and *Freundlich* isothermal

82 fitting constants of D-mag-MIPs.

Sorbents	Targets	$Q_{e,E}$ (mg/g)	<i>Langmuir</i> isothermal equation			<i>Freundlich</i> isothermal equation		
			R^2	$Q_{m,L}$ (mg/g)	K_L (mL/mg)	R^2	K_F (mL/mg)	n
D-mag-MIPs	DA	7.52	0.9936	8.7873	0.3671	0.9352	2.0422	0.5268
	DOPAC	8.16	0.9967	9.0334	0.6123	0.9396	2.8035	0.4473

83 $Q_{e,E}$ is the experimental value of Q_e ;

84 $Q_{m,L}$ is the calculated value of Q_e by *Langmuir* isotherm equation.

85

87 **Table S3.** The performance parameters of D-mag-MIPs-HLPC method for DA and

88 DOPAC detection. ($n=5$)

Analyte	Linearity range ($\mu\text{g/mL}$)	R^2	RSD (%)		LOD ($\mu\text{g/mL}$)	LOQ ($\mu\text{g/mL}$)
			intra-day	inter-day		
DA	0.10-100	0.9981	1.5-3.3	2.8-3.9	0.020	0.065
DOPAC	0.10-100	0.9987	1.6-3.1	2.3-3.6	0.031	0.096

Table S4. Comparison with other methods for detection of DA or DOPAC.

Analytical system	Linear range ($\mu\text{g/mL}$)	RSD (%)		LOD _{DA/DOPAC} ($\mu\text{g/mL}$)	Spiking concentration ($\mu\text{g/mL}$)	Sample	Recovery (%)	RSD (%)	Reusability	Magnetic Separation	Ref.
		intra-day	inter-day								
GEM ^a	0.61-15.3	--	--	0.404 / --	--/--	--	--/--	--/--	--	No	[35]
CS/N,GODs@SPCE ^b	0.16-15.3	0.9	--	0.023/ --	4.5	Human urine	~ 100	2.0	94.5 (after 1 month)	No	[36]
DE-MIPs ^c	0-0.183	--	--	0.023/--	3.0,1.2, 45.9, 91.8	Human serum	100.1-103.8	3.6-4.9	--	No	[37]
MISPE-HPLC-FL ^d	0.15-2.23	2.2-4.6	1.6-4.7	0.025/ --	0.15, 0.3, 0.76, 1.5, 2.3	Human urine	98.3-101.1	--	--	No	[38]
D-mag-MIPs-HPLC-UV	0.1-100	1.5-3.1	2.3-3.9	0.020/ 0.031	0.1, 1.0, 5.0	Human urine	95.5-98.6	2.7-5.1	91.0 (after 6 cycles)	Yes	This work

a: Graphene modified electrode.

b: Nitrogen-doped graphene quantum dots-chitosan nanocomposite-modified nanostructured screen printed carbon electrode.

c: Dual-emission fluorescent molecularly imprinted polymers.

d: Molecularly imprinted solidphase extraction.

